MAINTENANCE OF DYNAMIC STRAIN SIMILARITY AND ENVIRONMENTAL STRESS FACTOR IN DIFFERENT FLOW HABITATS: THALLUS ALLOMETRY AND MATERIAL PROPERTIES OF A GIANT KELP

A. S. JOHNSON* AND M. A. R. KOEHL

Department of Integrative Biology, University of California, Berkeley, CA 94720, USA

Summary

We have focused on the giant kelp *Nereocystis luetkeana* to examine the mechanical scaling of benthic marine organisms loaded in tension by hydrodynamic forces. If we consider simply the allometry of the kelp's morphological characters, we conclude that their stipes are underscaled relative to the blade area they support (i.e. that the kelp do not maintain stress or elastic similarity as they grow). However, a closer look at the characteristics of these kelp *in the field* reveals (1) that they have different blade shapes (and hence drag coefficients) and stipe material properties in different hydrodynamic environments, and (2) that they show a decrease in drag coefficient as they become larger. One consequence of these adjustments of blade and stipe morphology is that the maximum stresses in *N. luetkeana* stipes, when the kelp are pulled by peak tidal currents in their respective habitats, are similar for kelp of different sizes and for kelp from different sites. Hence, sessile organisms such as these kelp can, *via* their growth responses in different mechanical environments, show a phenomenon analogous to dynamic strain similarity. In addition, *N. luetkeana* also maintain a constant environmental stress factor, the ratio of the stress required to break a component of an organism (in this case the stipe) at some stage in its life to the maximum stress normally encountered in the habitat by that component during that stage (in this case, stress due to the drag on a kelp exposed to the peak tidal currents typical of the site at which it lives), both between habitats and as they grow.

Introduction

The consequences of body size for how organisms function has long intrigued biologists (reviewed in Alexander, 1971; Pedley, 1977; Banse and Mosher, 1980; McMahon and Bonner, 1983; Peters, 1983; Calder, 1984; Schmidt-Nielsen, 1984; Denny *et al.* 1985; Reiss, 1989; Patterson, 1992). Changes in body size are often accompanied by changes in shape, both during the ontogeny of an individual (e.g. Calder, 1984) and

*Present address: Department of Biology, Bowdoin College, Brunswick, ME 04011, USA.

during the evolution of a lineage (e.g. Gould, 1966; Bonner, 1968; Stanley, 1973). Most of the attention on how such shape changes affect the mechanical functioning of organisms has focused on the allometry of terrestrial creatures, whose support structures are loaded as buckling columns or bending cantilevers by their weight (proportional to volume) (e.g. McMahon, 1973, 1975). In contrast, little is known about the scaling of benthic aquatic organisms, for whom hydrodynamic forces are more important than gravity. The few studies of scaling that have examined benthic organisms have focused on structures loaded in bending or shear (e.g. Koehl, 1977; Denny *et al.* 1985); however, many benthic organisms are loaded in tension. Although some general rules have been proposed about how tensile structures such as kelp stipes (stems) should scale (Peterson *et al.* 1982), field measurements of how forces on these structures vary with size have not been made. Furthermore, although some investigators have recognized that the gaits used by locomoting animals can affect their mechanical scaling (e.g. Rubin and Lanyon, 1984), researchers have not yet explored the ways in which the responses of sessile organisms to environmentally induced loads might affect their scaling.

The overall goal of this study was to analyze the mechanical scaling of aquatic tensile biological structures. We focused our analysis on the stipes (stems) of the giant bull kelp *Nereocystis luetkeana* (Mertens) Postels and Ruprecht (see Fig. 1A).

Objectives

Scaling of tensile structures

A variety of biological structures (such as spider silk, fruit stems or the stipes of kelp with gas-filled floats) are loaded in simple tension. One objective of the present study was to measure how the load (F) on the stipe of a tensile aquatic macrophyte scales with the size of the organism and, in turn, how the dimensions of the stipe vary with respect to F.

If two structures are scaled to show 'stress similarity', then the stress (force per unit cross-sectional area of material bearing that force) at some position in the large structure is the same as the stress at a comparable position in the smaller structure when both perform the same function, such as supporting their own weight (e.g. McMahon, 1975). Structures of different sizes loaded in tension show stress similarity when $d \propto F^{0.5}$, where F is the force on the structure and d is its diameter (Peterson *et al.* 1982). Since stress in a tensile structure is simply force per unit cross-sectional area, diameter can be independent of length (Wainwright, 1970) as long as the weight of the tensile element is negligible relative to F.

If two structures are scaled to show 'elastic similarity' in bending, then the deflections of the large and small structures (normalized to their respective lengths) are the same when they perform comparable functions (McMahon, 1973). We define elastic similarity for a tensile structure as maintenance of $\Delta L/L$, where ΔL is the linear displacement of the end of the tensile structure as it is stretched by load F, and L is the length of the structure before F is applied. For a structure loaded in tension, extension per unit length is a function of stress (e.g. Wainwright *et al.* 1976); therefore, a tensile structure that maintains stress similarity also maintains elastic similarity.

While the force on a tensile fruit stem is proportional to the volume of the fruit,

Peterson *et al.* (1982) suggested that the force on a tensile kelp stipe is due to hydrodynamic drag on the blades (they assumed drag to be proportional to blade area, A_B). Therefore, they predicted that $d \propto A_B^{0.5}$. Although Peterson *et al.* (1982) did find that stipe diameter was independent of stipe length for the elk kelp *Pelagophycus porra,* they also found that stipe diameter appeared to be underscaled relative to blade area ($d \propto A_B^{0.268}$) for stress (and therefore, elastic) similarity.

We tested the assumption that the forces (F) on macrophytes are simply proportional to blade area (A_B), and we measured how the diameters (d) of the stipes scale with F. An organism in a unidirectional current is exposed to drag force (proportional to projected area), whereas an organism in ocean waves is also subjected to acceleration reaction force (proportional to volume) (Koehl, 1977; Denny *et al.* 1985). These hydrodynamic forces depend not only on the area or volume of the organism but also on the velocities and accelerations of the water flow in its habitat. Therefore, we measured the forces on kelp at similar velocities to those measured at the sites from which the kelp were collected.

Size-dependent material properties

A second objective of the present study was to incorporate measurements of size-dependent material properties into an analysis of mechanical scaling. The scaling models mentioned above have been based on the assumption that tissue material properties are independent of the size of an organism. This assumption, however, is invalid for many terrestrial plants (Niklas, 1992) and vertebrates (Currey, 1984) and some species of seaweed (Delf, 1932; Dudgeon and Johnson, 1992), all of which show changes in the mechanical properties of their support tissues as they grow and age.

Dynamic strain similarity

A third objective of the present study was to explore how the responses of kelp to different water flow environments might affect how the load (F) on the stipe scales with thallus (body) size. Rubin and Lanyon (1984) refined classical scaling ideas by considering the dynamic load imposed upon a structure during use. They found that during vigorous locomotion, the strains (for small deformations, strain is the change in length divided by the undeformed length) in the bones of vertebrates representing a range of body sizes were similar because large animals use gentler gaits than do small ones. They called this maintenance of peak functional strain independent of body size 'dynamic strain similarity'. The concept of dynamic strain similarity should also apply to non-locomoting creatures subjected to environmental forces (e.g. kelp in flowing water) if the organisms respond to the environment in ways that affect the magnitudes of such forces. For example, passive reconfiguration of sessile organisms in moving fluids can reduce drag (e.g. Koehl, 1977; Vogel, 1984). Furthermore, some sessile organisms can change the drag they experience by changing their shapes (*via* muscle contraction or growth) in response to their water-flow habitats (e.g. Koehl, 1977).

Environmental stress factor

A fourth objective of this study was to investigate whether aquatic macrophytes maintain their environmental stress factor as they grow in different water-flow habitats.

By 'environmental stress factor' we mean the ratio of the strength (σ_{brk}, the stress required to break the tissue) of a component of an organism at some stage in its life (in this case, the stipe of a non-senescent kelp sporophyte) to the typical maximum stress (σ_{max}) experienced by that component as it is used *day-to-day* in the habitat of the organism during that life stage (in this case, the stress in the stipe due to the maximum hydrodynamic force on the kelp during times of peak tidal current). In contrast, the safety factor of a component of an organism is the ratio of the strength of the tissue from which the component is made to the peak stress that it experiences *during its lifetime* (Alexander, 1981). For example, the environmental stress factor for a leg bone would be the ratio of the strength of the bone material in a healthy adult to the stress in the bone during running at peak velocity or jumping to maximum height. In contrast, the safety factor for that bone might be the ratio of the strength of the portion of the bone tissue most weakened by osteoporosis in an old animal to the stress experienced when that animal fell off a cliff.

There is variability within a population in the strength (σ_{brk}) of the support tissues of different individuals, and there is also variability in the peak stress (σ_{peak}) encountered by different individuals in their lifetimes. Therefore, the safety factor is often considered statistically, both for organisms and for man-made structures (see Alexander, 1981); such a statistical safety factor is the mean of the σ_{brk} values of the individuals in a population divided by the mean of the σ_{peak} values they encounter in their lifetimes. In practice, the safety factor is very difficult to determine because long-term field studies of the populations are required to determine how σ_{brk} values change with age. Similarly, measuring the lifetime σ_{peak} values experienced by members of a population can be a formidable undertaking, although Denny and Gaines (1990) and Denny (1991) have described how the statistics of extremes can be used to estimate peak forces on wave-swept organisms. In contrast, environmental stress factor is easier to determine because it involves measurements of the strength of an organism's tissues at a particular stage in its life and of the peak stresses experienced by those tissues as used by the organism at that stage in its habitat. Note that environmental stress factor can change with season and with the age of the organism, whereas safety factor represents the entire lifetime of the organism.

Several lines of evidence suggest that sessile organisms might be able to maintain a constant environmental stress factor or safety factor as they grow in different habitats. Some sessile marine organisms have been shown to change their breaking force (Etter, 1988; Palumbi, 1984) in response to their hydrodynamic environment, and some terrestrial plants have been found to maintain a constant safety factor as they increase in size (Tateno and Bae, 1990).

We have focused on the giant kelp *Nereocystis luetkeana* to determine how the thallus allometry, stipe material properties and blade responses to hydrodynamic environment affect environmental stress factors as the kelp grow in different water-flow habitats.

Nereocystis luetkeana

Nereocystis luetkeana sporophytes form extensive beds along the Pacific coast of North America, from California to Alaska. *N. leutkeana* blades, which can be up to 4 m

long, are held near the water surface by a gas-filled pneumatocyst atop a long, slim stipe attached to the substratum by a holdfast (Abbott and Hollenberg, 1976). These kelp, which occur in water about 3–17 m deep, are exposed to tidal currents and, in some habitats, to non-breaking waves (Koehl and Alberte, 1988).

N. luetkeana are essentially annual kelp: young sporophytes appear in the early spring, grow to the water surface by mid-summer, and wash away during winter storms (Rigg, 1917; Markham, 1969; Foreman, 1970; Nicholson, 1970; Vadas, 1972; Abbott and Hollenberg, 1976; Hawkes, 1981; Rosell and Srivastava, 1984; Wheeler *et al.* 1984; Miller and Estes, 1989), although a few individuals may persist through the winter (Rigg, 1917; Foreman, 1970; Rosell and Srivastava, 1984; Wheeler *et al.* 1984). *N. leutkeana* blades grow like conveyor belts: new tissue is added in the meristematic region near the blade base, sori (patches on the blades in which spores are produced) develop distally in older tissue, and sori are shed and old tissue is eroded at the blade tip. The main spore-producing season appears to be mid to late summer (Rigg, 1917): although spore production begins after the kelp reach the surface (Foreman, 1970; Duncan, 1973) and continues through autumn (Foreman, 1970; Abbott and Hollenberg, 1976; Amsler and Neushul, 1991), blade growth rate begins to slow in late summer (Wheeler *et al.* 1984), photosynthetic rate decreases (Rosell and Srivastava, 1984) and blades become badly frayed by winter (Foreman, 1970). Furthermore, epiphyte load on the blades increases from late summer into the winter (Peters, 1913; Rigg, 1917; Markham, 1969; Foreman, 1970; Nicholson, 1970; Hawkes, 1981; Rosell and Srivastava, 1984).

Materials and methods

Field sites

Nereocystis luetkeana were studied from three sites near San Juan Island, Washington, USA. The 'protected' site was a stretch of shore between Shady Cove and Cantilever Point near Friday Harbor Laboratories that experienced peak velocities of $0.5\,\mathrm{m\,s^{-1}}$ (maximum tidal current plus maximum velocity fluctuation measured during a storm, Koehl and Alberte, 1988). The 'current-swept' site was Turn Rock in San Juan Channel that experienced peak velocities of $1.5\,\mathrm{m\,s^{-1}}$ (the maximum tidal current at this site during a year was $1.1\,\mathrm{m\,s^{-1}}$ (National Oceanic and Atmospheric Administration, 1981); the maximum velocity fluctuation measured during a storm at this site was $0.4\,\mathrm{m\,s^{-1}}$ (Koehl and Alberte, 1988)). The 'wavy' site was Cattle Point, which was subjected to small waves superimposed on tidal currents; daily peak velocities ranged between 0.6 and $1.7\,\mathrm{m\,s^{-1}}$ on non-stormy days at a site about 100 m from ours (D. Pentcheff, unpublished data; recorded over nine separate days, April–July).

N. luetkeana were collected from the kelp bed at each of the sites described above. A boat was anchored at two haphazardly selected positions at Turn Rock (one near the edge and another near the middle of the bed), and all the kelp within reach of the boat at each position were collected. This technique was also used to sample kelp from Shady Cove, but because the kelp bed was narrow at this site, there was no distinction made between the edge and the middle of the bed. Kelp at Cattle Point were collected by wading from the shore to a haphazardly selected point in the middle of the kelp bed; all kelp

encountered within 1 m of a transect run from that point parallel to the shore were taken until the collecting bags were full. Collections were made at Shady Cove on August 23 and September 29, at Turn Rock on July 19, and at Cattle Point on July 6, 1982.

Drag measurements

The drag (D) on individual *N. luetkeana* was determined (Koehl and Wainwright, 1985) to the nearest 0.1 N using an Ametek model LKG5 force gauge. Each kelp was towed just below the water surface at a number of different velocities (measured with a Marsh–McBirney model 511 electromagnetic flow meter) outside the wake of a boat. We focused on velocities at the high end of the range encountered *in situ* to examine the susceptibility of kelp to breakage by currents: *N. luetkeana* from the protected and the wavy sites were towed at 0.25, 0.50 and 0.75 m s^{-1}, and kelp from the current-swept site at 0.50, 1.00 and 1.50 m s^{-1}.

Drag (D) on large objects in rapidly flowing water is given by:

$$D = \frac{1}{2}\rho U^2 S C_D, \tag{1}$$

where ρ is the density of the water, U is the velocity, S is a relevant plan area of the body (in our case, projected area of the blades, A_B, plus projected area of the stipe and pneumatocyst of a kelp) and C_D is the drag coefficient, which depends on body shape (in our case, the lower the C_D of a kelp, the more 'streamlined' its bundle of blades).

Morphological measurements

Each morphological variable quantified in this study (shown in Fig. 1 and described below) was measured at least three times to determine the precision of our techniques. Symbols used to characterize morphology throughout the manuscript are listed in Table 1.

Blade characteristics

All blades on a kelp were removed, spread out along with grids marked in cm^2, and photographed from an overhanging balcony one storey (3.5 m) above them. The resulting slides were projected onto paper and the perimeter of each blade was traced. Vernier calipers were used to measure blade length (L_B) and blade width (W_B) at the widest part of the blade on these tracings (Fig. 1B); these measurements were made to the nearest millimeter after conversion. Since there were several tiny or broken blades on each kelp, the mean length and width of only the longest 50 % of the blades on each kelp was used to characterize the L_B and W_B for each kelp. The projected areas of the blades were measured to the nearest 0.001 m^2 by weighing paper cut-outs of the tracings. The total blade projected area (A_B) for a kelp was calculated by summing the areas of all of the blades of the kelp. To obtain an estimate of the error in our first method (see *Allometric analysis* below), projected area measurements were repeated on seven of the kelp (ranging in size from 0.1 to 2.3 m^2) using another technique: the slides of blades were projected onto a digitizing tablet (Jandel model 220/2210) interfaced with a Toptec XT computer, and their areas were calculated using Sigma-Scan software (Jandel Scientific).

Stipe and holdfast characteristics

Stipe diameter was measured to the nearest millimeter using vernier calipers at the holdfast (d_1) (see Fig. 1D), and at 15 cm intervals (l_A, measured with a ruler) along the entire length of the stipe; stipe diameter (d_N) just proximal to the pneumatocyst was also measured. Stipe length (L_S) was determined to the nearest centimeter by summing the values of l_A for the entire stipe plus l_N and the length of the pneumatocyst (see Fig. 1D,F). The narrowest stipe diameter (d) measured for each kelp was used in subsequent statistical comparisons, for calculation of stress due to drag (see below) and for scaling arguments.

The volume of the gas-filled cavity (V_G) in each *N. luetkeana* from Turn Rock and Shady Cove was determined by cutting the kelp transversely at the position of d_N (Fig. 1D), filling the pneumatocyst and the stipe cavities with water, and then measuring the volume of this water to the nearest milliliter using a graduated cylinder.

Total tissue volume (V) of each stipe (Fig. 1F) was determined as follows. Total volume for the proximal portion of the stipe was estimated by:

$$V = \pi l_A (d_1^2 + d_2^2 + d_3^2 + ... d_N^2)/4 \, , \tag{2}$$

where l_A is 15 cm, d_1 is the diameter of the stipe closest to the holdfast, d_2 is the diameter of the next 15 cm section of the stipe and d_N is the diameter of the most distal 15 cm segment of the stipe. Total volume for the most distal segment of the stipe closest to the pneumatocyst was estimated by:

$$\text{total volume of last segment} = \pi l_N (d_N^2)/4 \, , \tag{3}$$

where l_N is the length of the last segment, and that of the pneumatocyst was estimated by:

$$\text{total volume of pneumatocyst} = \frac{4}{3} \pi (d_p/2)^3 \, , \tag{4}$$

where d_p is the diameter of the pneumatocyst (Fig. 1B). Total tissue volume of the stipe was then determined as the sum of these three volumes (from equations 2–4) minus the gas volume of the pneumatocyst and stipe (determined as described above).

The areas of intact, undamaged holdfasts (H) were determined for kelp from Cattle Point and Shady Cove (no undamaged holdfasts were available for kelp from Turn Rock). The longest dimension (H_a) of each holdfast, as well as the width (H_b) of the holdfast perpendicular to H_a were measured to the nearest 0.5 cm with a ruler (Fig. 1E). Holdfasts were assumed to be elliptical and their areas were calculated using H_a and H_b as the major and minor axes.

Principal components analysis

To compare the morphologies of the kelp from different sites, we used principal components analysis (Chatfield and Collins, 1980) to summarize a number of the variables we measured to characterize stipe morphology (stipe length and stipe smallest diameter) and blade morphology (total projected blade area, blade length, blade width and drag, which depends on blade ruffliness as well as size; Koehl and Alberte, 1988). The principal components analysis was performed using SPSSX software (version 9; SPSS, Inc) on a VACS mainframe computer. Each principal component represents a linear summary
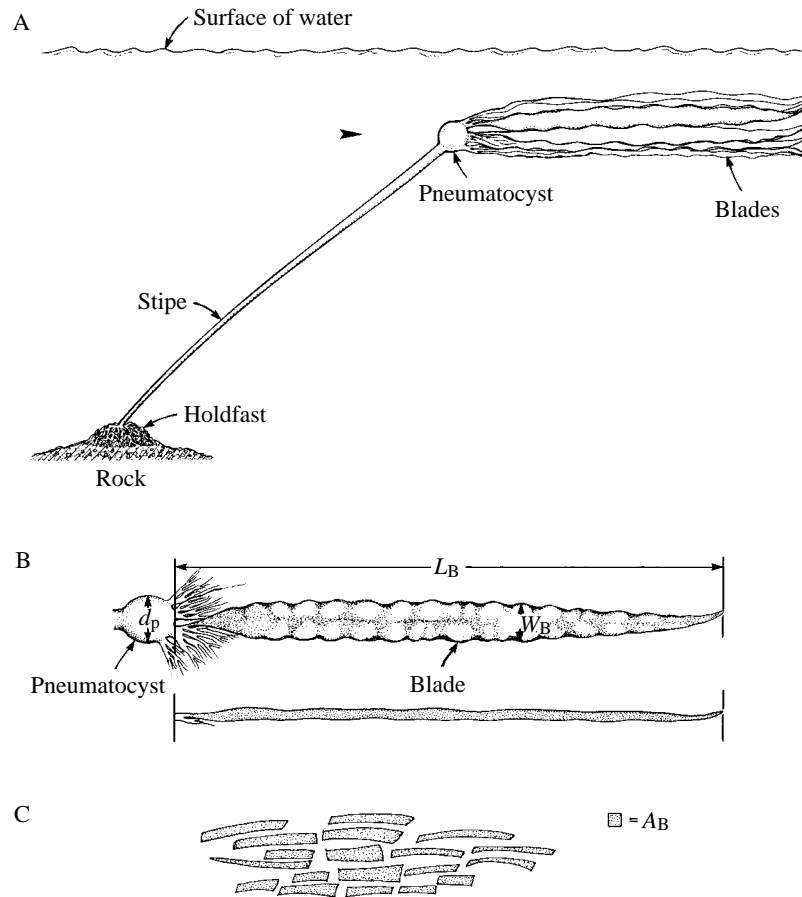
Fig. 1. Diagram of morphological features of *Nereocystis luetkeana*. (A) Diagram of a kelp *in situ* in a gentle current (direction indicated by arrowhead). (B) Top view of the pneumatocyst (of diameter d_P) and one of the ruffled blades of a kelp from the protected habitat (Shady Cove); blade length (L_B) and greatest blade width (W_B) are indicated on this diagram. The narrower, flatter blade diagrammed below is typical of those from kelp at the current-swept site (Turn Rock). The projected area of each blade is the area within the line drawn that indicates the edge of the blade; blade area (A_B) for a kelp is the sum of such projected areas for all the blades on the kelp. (C) Diagram of a ruffled blade cut into pieces that lie flat. The sum of the areas (indicated by stippling) of all these pieces is the actual plan area of the blade, A_B. Dividing actual area by projected area (see B) for a blade gives the 'ruffliness index' used by Koehl and Alberte (1988), which was 1.09 for *N. luetkeana* from our protected site and 1.00 for kelp from our current-swept site.

(similar to a linear multiple regression) of the data that combines several variables into one descriptive variable (the principal component). Several principal components can be constructed from each set of variables. The first principal component is the linear equation for the line that best fits the data; that is, that accounts for most of the variation. The second principal component is the line constructed from the data, perpendicular to the first principal component, that accounts for most of the remaining residual variation.
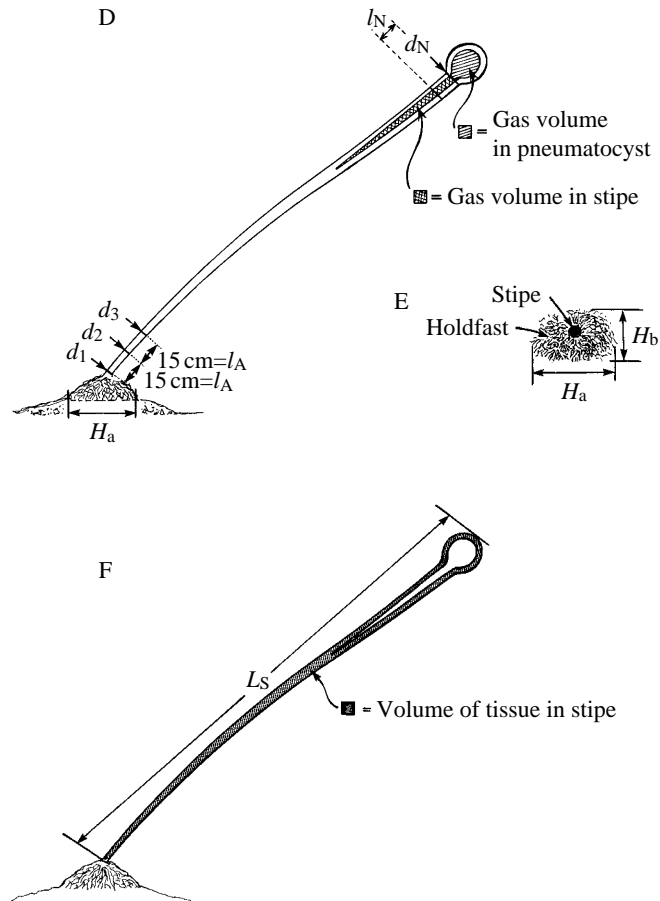
(D) Diagram of the stipe of a *N. luetkeana* bisected longitudinally. H_a, greatest width of holdfast; d_1, diameter of stipe just above holdfast; d_2, diameter of stipe 15 cm distal to d_1; l_A, a section of stipe 15 cm in length; d_N, diameter just proximal to the pneumatocyst; l_N, the length of the most distal segment (measured to d_N). Hatched area indicates the gas-filled space in the pneumatocyst and cross-hatched area indicates the gas-filled space in the stipe. (E) Top view of the holdfast of a *N. luetkeana*, with the stipe shown in cross-section. H_a, greatest width of holdfast; H_b, width of holdfast perpendicular to H_a. (F) Diagram of a kelp bisected longitudinally, with the hatched area indicating the tissue volume of the stipe plus pneumatocyst. L_S, total length of the stipe plus pneumatocyst.

Principal components analysis not only allows us to summarize many variables with only one or two new variables (principal components), but it also allows us to look for patterns in the clumping of the data when the principal components that are derived from the data are plotted against one another.

Mechanical properties of stipe tissues

Mechanical properties of stipe tissues (material properties; symbols listed in Table 2) from each kelp were measured by conducting tensile tests using techniques described by Koehl and Wainwright (1977, 1985). These tests were conducted on a Houndsfield
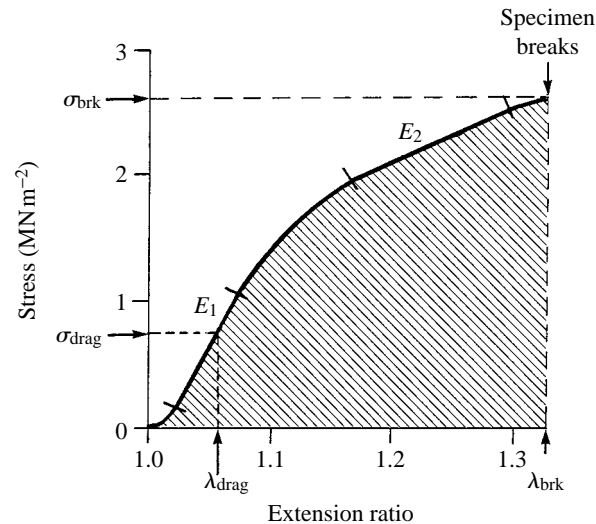
Fig. 2. Plot of stress (σ) as a function of extension ratio (λ) for a piece of the stipe of *N. luetkeana* from the protected site subjected to a tensile test. σ_{brk}, stress required to break the stipe; λ_{brk}, extension ratio required to break the stipe; σ_{drag}, stress in the stipe due to drag on the kelp in a current of specific velocity; λ_{drag}, extension ratio due to this drag; E_1, elastic modulus of the stipe tissue at low λ; E_2, elastic modulus at high λ. The hatched area under the curve indicates the work per tissue volume (W/V) required to break the specimen.

Tensometer, model W, arranged to record force and extension electronically as described by LaBarbera (1985). Tests were carried out on at least three replicate pieces of stipe taken from the end nearest the holdfast, where kelp *in situ* usually break (Foreman, 1970; M. A. R. Koehl, personal observation). Material properties were only determined for specimens that did not slip or break at the tensometer grips. When more than one test was successful for a kelp, we used the mean value for that kelp. The pre-test length between the grips of each specimen (L_0), which was measured to the nearest 0.1 mm with vernier calipers, was between 11 and 14 cm. Stipe specimens were cylindrical, and the diameter of the narrowest portion of each was measured to the nearest 0.1 mm using vernier calipers; cross-sectional areas (A_0) were calculated using this diameter. Strain rates (strain rate=$(\Delta L/L_0)/t$, where ΔL is the increase in length of the specimen as it is pulled, and t is the time interval over which ΔL occurred) ranged from 0.025 to 0.084 s^{-1}; strain rate within this range had no significant effect (i.e. $P>0.05$; linear regression analysis) on any of the material properties used in our analysis. [Note that a test for zero slope is unbiased in the presence of error in the independent variable (Fuller, 1987). Therefore, no correction of slope was necessary for this result.]

The material properties we calculated are illustrated in Fig. 2. The extension ratio (λ) of the specimen is given by:

$$\lambda = (\Delta L + L_0)/L_0, \tag{5}$$

and the stress (σ) is given by:
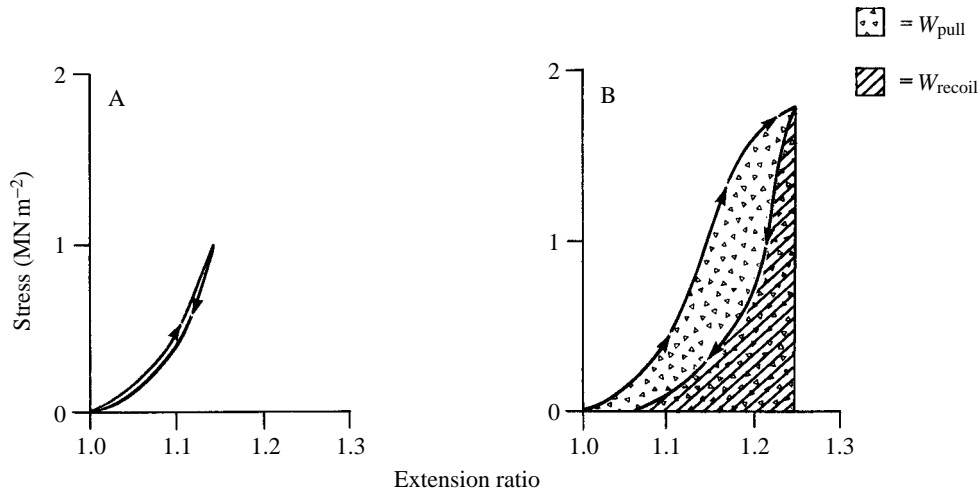
$$\sigma = F/A_0, \tag{6}$$

Fig. 3. Plots of stress (σ) as a function of extension ratio (λ) for pieces of the stipe of *N. luetkeana* from the protected site subjected to tensile tests in which they were pulled to a given value of λ and then returned at the same rate to their original length. (A) Example of a stipe specimen pulled to a value of λ within the E_1 region of the σ/λ curve. (B) Example of a stipe pulled to a value of λ within the E_2 region of the σ/λ curve. The stippled area represents the work per volume required to pull the specimen (W_{pull}), and the hatched area represents the work per volume stored in the tissue and used for elastic recoil (W_{recoil}).

where F is the force with which the specimen resists that extension. The stress at which a specimen broke (σ_{brk}) is a measure of the strength of the stipe tissue, and the extension ratio at which it broke (λ_{brk}) is a measure of its extensibility. The area under a plot of stress as a function of extension ratio for a specimen pulled until it broke is the work per volume (W/V) required to break that specimen. The slope (E) of a plot of stress *versus* extension ratio of the tissue is a measure of the stiffness of the material. We call the slope of the straight portion of the stress/extension ratio curve for *N. luetkeana* stipe tissue at low extensions 'modulus 1' (E_1) and the slope of the straight portion of the curve at high extensions 'modulus 2' (E_2).

We also conducted a series of stress–extension tests in which we pulled *N. luetkeana* stipes to various extensions and then returned them to their initial lengths (L_0). The area under a plot of stress *versus* extension ratio for a specimen being pulled is a measure of the work (W_{pull}) per volume required to stretch the specimen to a given extension ratio, while the area under the curve as the specimen is being brought back to L_0 is a measure of the strain energy (W_{recoil}) stored in the specimen available for elastic recoil (Fig. 3B). A measure of the resilience of stipe tissue is W_{recoil}/W_{pull}. Such resilience measurements were conducted for *N. luetkeana* collected from the protected site during the summer of 1975.

Site-specific mechanical features

We used estimates of typical peak velocities for the two sites subjected to unidirectional currents ($0.5\,\mathrm{m\,s^{-1}}$ for the protected site and $1.5\,\mathrm{m\,s^{-1}}$ for the current-

swept site, as described above in the section on field sites) to determine the 'peak drag force' on each kelp *in situ*. The peak drag on each kelp was divided by the narrowest cross-sectional area of the stipe of that kelp to yield an estimate of the peak stress due to drag in the stipe of each kelp (σ_{drag}, Fig. 2). The extension ratio corresponding to that stress was determined from each stress/extension ratio curve for that kelp, and the mean of those extension ratios for each kelp was used as an estimate of the peak extension ratio due to drag experienced by that kelp *in situ* (λ_{drag}, Fig. 2). For each curve, we noted whether the point on the curve defined by (σ_{drag}, λ_{drag}) fell in the region of E_1 or E_2 (defined above; Fig. 2).

The environmental stress factor (ESF) for each kelp was estimated as $\sigma_{brk}/\sigma_{drag}$, where σ_{brk} is the mean breaking stress of the stipe tissue of that kelp.

To compare how kelp from different sites might fare under the same flow conditions, we also calculated the σ_{drag} and the λ_{drag} for a velocity of $0.5\,\mathrm{m\,s^{-1}}$ for each kelp from each of the three sites.

Allometric analysis

Scaling relationships between various morphological and drag variables were examined by applying standard allometric analysis (e.g. Alexander, 1971; Schmidt-Nielsen, 1974, 1984). Since these allometric relationships are represented by exponential equations, we analyzed double logarithmic plots of the various variables. The equation of the line for such a plot is:

$$\log y = \log a + b \log x, \tag{7}$$

where b (the slope of this linear equation) is the exponent that expresses the relationship between the rate of increase in y per unit increase in x.

Standard least-squares linear regression will generally underestimate the slope (b) for allometric relationships with a low r^2 because of error in the measurement of the independent variable (LaBarbera, 1989). Reduced major axis estimates are often used to avoid such underestimation of the slope; however, the use of reduced major axis is not recommended because it can yield meaningless results, such as a slope between two uncorrelated variables (Harvey and Pagel, 1991). Alternatively, the effect on the slope of the error in the independent variable can be estimated if the measurement error of the independent variable is known. We used the reliability ratio, κ (where $\kappa = r$, and r is the correlation between repeated measurements of a variable; Fuller, 1987) to estimate the measurement error in our independent variables, and then used this κ to correct the slopes of our regression lines, as described below. To determine κ for drag measurements, we made three separate measurements of drag on each kelp, and we compared regressions of the first set with those for the second and the first set with the third set. The value κ was calculated as the mean r for these two regressions. To determine κ for blade area, we measured blade area using two different techniques (described above) and calculated the regression of the results of technique one with those of technique two. The value κ was determined from the r for this regression. We calculated the corrected slope (β) by multiplying the uncorrected slope (b) of the double logarithmic plot by $1/\kappa$ for plots of stipe diameter as a function of drag and of stipe diameter as a function of blade area.

Analyses of variance (ANOVAs), *t*-tests, Kendal's τ and linear regression analyses were performed using StatView software (version 1.03; Abacus Concepts, Inc.) on a MacIntosh IIci. Homogeneity of variances was tested using the F_{max}-test. Analysis of covariance (ANCOVA) comparisons were performed using ANCOVA software created by R. Etter (version 1.0).

Results and discussion

In this section we will discuss the allometry of *N. leutkeana* in different habitats, but will then move beyond this standard morphological scaling analysis to consider how the kelp actually perform in the field. To this end, we will first incorporate measurements of the hydrodynamic forces on the kelp into our scaling analysis, and we will then determine whether stipe material properties change with size or habitat. All these data will then be used to consider whether *N. leutkeana* in diverse habitats show dynamic strain similarity and whether they are scaled in such a way as to maintain a constant environmental stress factor. First, however, we must consider the seasons for which our data for *N. luetkeana* are relevant.

Deterioration of kelp in the autumn

As described in the Introduction, *Nereocystis luetkeana* are generally considered to be annual kelp, the main source of mortality being breakage during autumn and winter storms. To examine whether changes in morphology or material properties occurred as kelp were damaged or removed from a kelp bed in the autumn, we measured autumn kelp as well as summer kelp at the protected site (the site that was most easily accessible during bad weather). We found no significant difference in the material properties of stipe tissues between kelp collected in May at this site (data from Koehl and Wainwright, 1977) and those of kelp collected in August (*t*-tests, all *P*>0.10). However, by the end of September, the population of kelp remaining at this site were shorter (Table 1) and their stipe tissues had lower breaking stresses, elastic moduli and *W/V* ratios (Table 2) than did summer kelp. The autumn kelp were also more abraded and bore a heavier load of epiphytes. Therefore, except for those variables whose values did not change between August and September, all between-site comparisons were made using only data for healthy summer kelp from each site.

Morphological comparisons of kelp from different sites

Blade morphology

N. luetkeana at the current-swept site had flat, narrow, very long strap-like blades, whereas those at the protected site had significantly wider (Table 1), undulate (i.e. ruffled) blades (Fig. 1B,C). This pattern of strap-like blades in current-swept habitats *versus* ruffled blades in protected habitats has already been reported for *N. luetkeana* (Koehl and Alberte, 1988), as well as for a number of other species of macroalgae (reviewed in Koehl and Alberte, 1988; McEachreon and Thomas, 1987; Armstrong, 1989; Jackelman and Bolton, 1990; Gutierrez and Fernandez, 1992). These blade shape differences in *N. luetkeana* (M. A. R. Koehl, unpublished data) and *Laminaria*

Table 1. *Mean morphological variables of* Nereocystis luetkeana

Variable	Symbol	Site		
		Protected	Wavy	Current-swept
Blade projected area (m^2) (total for a kelp)	A_B	1.31±0.27 (18) ———————————*	0.66±0.22 (23)	2.13±0.63 (9) ————————
Blade width (m)	W_B	0.093±0.006 (18)	0.051±0.005 (23)	0.043±0.005 (9)
Blade length (m)	L_B	Aug. 2.08±0.44 (7) Sept. 1.13±0.16 (11)	0.86±0.12 (23)	1.94±0.30 (9)
Stipe diameter (mm)	d	5.3±0.36 (18)	5.3±0.41 (23)	6.0±0.86 (9)
Stipe length (m)	L_S	Aug. 5.32±0.89 (7) Sept. 3.18±0.36 (11)†	1.76±0.24 (23)	4.16±0.28 (9)
First principle component	PC1	Aug. 3.90±1.60 (7) Sept. 0.44±0.69 (11)	−1.88±0.62 (20)	1.45±1.22 (9)
Second principal component	PC2	0.36±0.15 (18)	0.32±0.17 (20)	−1.3±0.13 (9)
Pneumatocyst diameter (cm)	d_p	Aug. 6.63±0.66 (7) Sept. 5.36±0.27 (11)	4.58±0.23 (21)	6.91±0.43 (9)
Holdfast area (m^2)	H	Aug. 0.69±0.18 (5) Sept. 0.20±0.11 (7)†	0.33±0.12 (20)	NA
10^4×volume of gas-filled cavity (m^3)	V_G	3.7±0.80 (18)	‡	4.6±1.2 (9)
10^3×tissue volume (m^3)	V	Aug. 1.39±0.34 (7) Sept. 0.56±0.13 (11)†	‡	1.26±0.36 (9)

Values are mean ± S.E.M; numbers of kelp are given in parentheses.

ANOVA was used to compare means between sites; Fisher PLSD was used for *a posteriori* pairwise comparisons.

Values underlined with the same type of line along a row are not significantly different ($P<0.05$) except as indicated by asterisks.

For the protected site, separate means for the months of August and September are given if they were significantly different from each other; otherwise, only one pooled mean for both months is given.

*The values for the wavy and current-swept sites were significantly different from each other, but neither was different from those at the protected site.

†Although the August and September values for the protected site were significantly different from each other, neither was different from the values for other sites that are also underlined.

‡Float volumes were not measured for the kelp from the wavy site; hence, tissue volumes could not be calculated.

saccharina (Gerard, 1987) are due to plastic growth responses to tensile loads on the blades.

Kelp at the wavy site showed an intermediate morphology: they were undulate, but narrow (Table 1). Since long, flexible kelp in the oscillatory flow associated with waves move *with* the flow and experience little force before the flow direction reverses (as explained in Koehl, 1984, 1986; and measured by Koehl *et al.* 1991), it is not surprising that these long kelp moving back and forth in small waves showed the 'protected' type of undulate blade morphology.

Stipe morphology

The morphology of stipes from *N. luetkeana* at all three sites was quite similar.

Table 2. *Mean mechanical variables of* Nereocystis luetkeana

Variable	Symbol	Site		
		Protected	Wavy	Current-swept
Breaking stress (MN m^{-2})	σ_{brk}	Aug. 4.99±0.74 (7)	2.77±0.14 (17)	2.92±0.23 (9)
		Sept. 1.39±0.07 (11)		
Breaking extension ratio	λ_{brk}	1.31±0.02 (18)	1.35±0.03 (17)	1.30±0.03 (9)
Stiffness 1 (MN m^{-2})	E_1	Aug. 38.0±4.87 (7)	18.8±1.37 (22)	16.6±1.08 (9)
		Sept. 10.5±0.78 (11)		
Stiffness 2 (MN m^{-2})	E_2	Aug. 8.83±1.05 (7)		8.33±1.51 (9)
		Sept. 2.78±0.28 (11)	5.80±0.33 (18)	
Work to break per volume (MJ m^{-3})	W/V	Aug. 1.11±0.21 (7)		
		Sept. 0.25±0.03 (11)	0.517±0.07 (16)	0.464±0.07 (9)
Total work to break kelp (kJ)	W	Aug. 1.56±0.40 (7)	*	
		Sept. 0.143±0.035 (7)		0.539±0.137 (9)
Stress due to drag (MN m^{-2}) (0.5 m s^{-1})	$\sigma_{drag(0.5)}$	0.62±0.08 (18)	0.31±0.04 (20)	0.17±0.03 (9)
Extension ratio due to drag (0.5 m s^{-1})	$\lambda_{drag(0.5)}$	Aug. 1.029±0.005 (7)	1.039±0.003 (21)	1.031±0.003 (9)
		Sept. 1.075±0.011 (7)		
Stress due to drag (MN m^{-2}) (site-relevant)	σ_{drag}	0.62±0.08 (18)	†	0.61±0.09 (9)
Extension ratio due to drag (site-relevant)	λ_{drag}	Aug. 1.029±0.005 (7)	†	
		Sept. 1.075±0.011 (7)		1.061±0.003 (9)
Environmental stress factor (site-relevant)	ESF ($\sigma_{brk}/\sigma_{drag}$)	Aug. 11.6±3.02 (7)	†	6.50±1.85 (9)
		Sept. 3.23±0.75 (7)		

Values are mean ± S.E.M.; numbers of kelp are given in parentheses.

ANOVA was used to compare means between sites; *a posteriori* pairwise comparisons were done using the Fisher PLSD.

Values underlined with the same type of line along a row are not significantly different ($P<0.05$).

For the protected site, separate means for the months of August and September are given if they were significantly different from each other; otherwise, only one mean, obtained by pooling values for both months, is given.

*Data on stipe tissue volume could not be calculated for the kelp from the wavy site (see Table 1).

†Since kelp from the wavy site were not exposed to steady drag, we could not calculate site-relevant σ_{drag}, λ_{drag} or ESF.

Although other brown macrophytes have been found to have wider stipes (Rice *et al.* 1985) or larger holdfasts (Norton, 1986) in exposed habitats, there was no significant difference between the narrowest stipe diameters or between the holdfast areas (Table 1) of *N. luetkeana* from different flow habitats. Furthermore, even though the current-swept kelp had larger blade areas than did the protected kelp, there was no significant difference between these sites in the volume of the gas-filled cavity (Fig. 1D) that provides the buoyancy to hold the blades near the water surface. In contrast, stipe length did vary between sites, being significantly lower at the wavy site. *N. luetkeana* stipes grow in length until the blades approach the water surface (Hurd, 1916; Foreman, 1970; Nicholson, 1970; Duncan, 1973; Duncan and Foreman, 1980); hence, the shorter stipes at the wavy site simply reflected the fact that the water was shallower at this site.
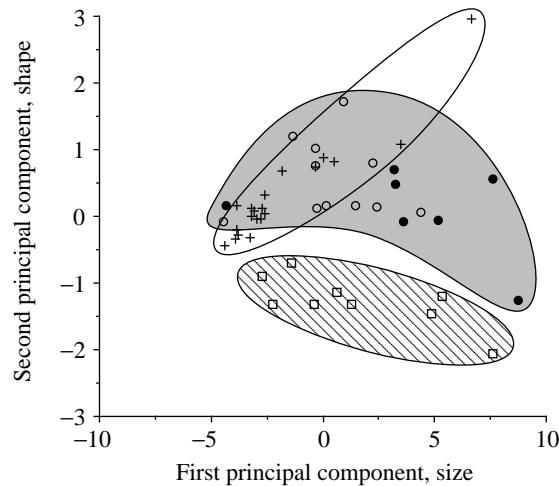
Fig. 4. Plot of the second principal component (PC2, a shape factor) as a function of the first principal component (PC1, a size factor) for all kelp used in this study, as explained in the text. Filled circles (●) indicate summer kelp from the protected site, open circles (○) indicate autumn kelp from the protected site, open squares (□) indicate kelp from the current-swept site, and crosses (+) indicate kelp from the wavy site. We have encircled the clusters of points for each of the three sites: the hatched area indicates the current-swept site, the stippled area indicates the protected site and the clear area indicates the wavy site. Separate linear regression analyses of PC2 as a function of PC1 at each site reveal patterns of shape change that occur with size. The shape of kelp at the protected site was independent of their size (linear regression analysis: summer protected, $P=0.41$; autumn protected, $P=0.96$). However, contrasting shape changes occurred with size at the other two sites: there was a negative association between PC1 and PC2 at the current-swept site (linear regression analysis: $P=0.02$, $r^2=0.48$) and a positive association between PC1 and PC2 at the wavy site (linear regression analysis: $P=0.0001$, $r^2=0.91$).

Principal components analysis

The morphological features of kelp from the different sites were summarized using principal components analysis, as described in Materials and methods section. We included drag force (D) in the principal components analysis because drag reflects the morphology of the blades (large size and high degree of 'ruffliness' result in high drag; Koehl and Alberte, 1988). The first principal component ($PC1 = 0.89L_B + 0.87W_B + 0.77D + 0.75d + 0.75L_S + 0.65A_B$) accounted for 61 % of the variation in these variables, while the second principal component ($PC2 = 0.55W_B + 0.50D + 0.14d - 0.30A_B - 0.34L_B - 0.37L_S$) accounted for 15 % of the variation in these variables (abbreviations defined in Table 1). The two variables that carried the most weight in the first principal component (L_B, W_B) are both related to the size of the blades, so we call PC1 the 'size variable'. The two variables that carried the most weight in the second principal component (W_B, D) are both related to blade shape (wide blades are undulate in shape, and blades with high drag are undulate; Koehl and Alberte, 1988), so we call PC2 the 'shape variable'.

A plot of PC2 as a function of PC1 (Fig. 4) shows that kelp from different sites cluster in different regions of this morphospace. Kelp from the shallow wavy site were smaller

(had significantly lower PC1 values) than were those from the other two deeper sites, and autumn kelp were significantly smaller than summer kelp from the protected site. Blades at the current-swept site were flatter and narrower (had significantly lower PC2 values) than were those at the other two sites (Table 1).

The relationship of PC2 to PC1 gives a rough summary of how shape changes with size for *N. luetkeana* from the different sites. Shape was independent of size for kelp from the protected site, whereas PC2 increased with size for kelp from the wavy site (for interpretation, see discussion of blade morphology above). In contrast, at the current-swept site, larger kelp had lower PC2 values (i.e. had flatter, narrower blades) than did smaller kelp (statistics reported in Fig. 4). Hence, at the current-swept site, where hydrodynamic forces on *N. luetkeana* are likely to be the largest, the kelp took on a more streamlined blade morphology as they grew (see discussion of drag below).

Allometry

Since a *N. luetkeana* stipe is a tensile structure, stipe diameter would not be expected to scale with stipe length (Wainwright, 1970; Peterson *et al.* 1982). Indeed, we found that stipe diameter was independent of stipe length at all three sites (linear regression analysis: current-swept, $P=0.59$, $N=9$; wavy, $P=0.24$, $N=21$; summer protected, $P=0.35$, $N=7$; autumn protected, $P=0.49$, $N=11$).

For both elastic similarity and stress similarity between small and large tensile structures, the diameter of the structure should be proportional to the force on the structure raised to the power 0.5 (Peterson *et al.* 1982). Since the mechanical load on the stipe of a *N. luetkeana* is due to the drag force on the blades of the kelp (Koehl and Wainwright, 1977), stipe diameter might be expected to scale with $A_B^{0.5}$ (Peterson *et al.* 1982). The results of our analysis, however, indicate that, according to this criterion, stipe diameter (d) is underscaled with respect to blade area (A_B) at all sites: at the protected site, $d \propto A_B^{0.1}$; at the wavy site, $d \propto A_B^{0.2}$; and at the current-swept site, $d \propto A_B^{0.3}$ (Fig. 5). All these exponents are significantly less than 0.5 (statistics reported in Fig. 5). Similarly, Peterson *et al.* (1982) found for the stipes of the elk kelp *Pelagophycus porra* that $d \propto A_B^{0.268}$, and several species of red algae also show such underscaling of stipe diameter with blade area (Carrington, 1990; Dudgeon and Johnson, 1992). Thus, it appears that *N. luetkeana* stipe diameters do not increase enough as the kelp grow to maintain elastic or stress similarity and that this underscaling is most pronounced at the more protected site.

Although the preceding analysis suggests that *N. luetkeana* are not scaled according to elastic or stress similarity, this analysis was based on the commonly used assumptions that (1) the mechanical load on the structure was proportional to some morphological variable (in our case, blade area), and (2) the structure's material properties were constant. In the following sections, we will explore the validity of each of these assumptions.

Drag

Drag on kelp of different morphologies and sizes

At a given velocity, *N. luetkeana* from the current-swept site experienced lower drag than did kelp of comparable blade area from the protected or the wavy habitats (Fig. 6A).
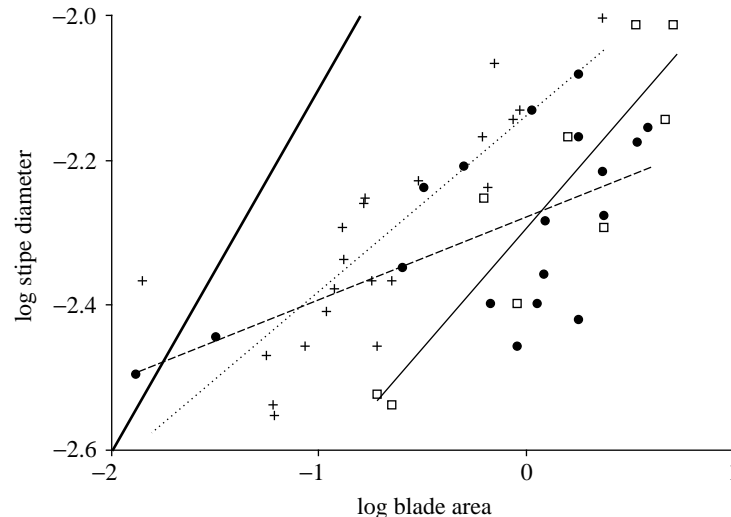
Fig. 5. Double logarithmic plot of stipe diameter (d) (in m) as a function of blade area (A_B) (in m^2) for kelp from each site: protected (filled circles, dashed line, slope=0.11, P=0.01, r^2=0.31), current-swept (open squares, solid line, slope=0.33, P=0.001, r^2=0.79) and wavy (crosses, dotted line, slope=0.24, P=0.0001, r^2=0.67). Slopes are uncorrected for error in measurement of blade area because the value obtained for κ was 0.999. t-tests revealed that all slopes are significantly less than 0.5 (the slope of the thick solid line: protected, P<0.001; current-swept, P<0.05; wavy, P<0.001). ANCOVA revealed that the slopes differ from each other (P<0.05). *A posteriori* tests using Tukey's Q revealed that the slope of the line obtained for the protected site was significantly less than those of the other two sites (P<0.05), but that there was no difference in slopes obtained from the current-swept and wavy areas (P>0.05). Note that there was no significant difference between either slopes or y-intercepts of regression lines calculated for all the kelp from the protected site or for kelp from the protected site excluding the two smallest kelp (ANCOVA, $P \gg 0.05$).

The C_D values of *N. luetkeana* (Fig. 7) are similar to those reported for other species of deformable seaweeds (e.g. Denny, 1988; Carrington, 1990; Dudgeon and Johnson, 1992). The current-swept kelp were more streamlined (i.e. had lower drag coefficients, C_D; Fig. 7) than those from the other sites because the narrow, flat blades on a current-swept kelp flapped with lower amplitude and collapsed together into a narrower bundle in flowing water than did the undulate blades of kelp from the other sites. (This phenomenon was quantified by Koehl and Alberte, 1988.) While several other studies of macroalgae have also shown that thallus shape affects drag (Armstrong, 1987; Koehl and Alberte, 1988; Sheath and Hambrook, 1988; Dudgeon and Johnson, 1992), Carrington (1990) found that shape did not affect C_D values of very collapsible seaweeds at the high velocities characteristic of shores exposed to large breaking waves.

Vogel (1984) has proposed a number called the 'figure of merit' (B) to describe the relative reduction in drag experienced by flexible structures as they reconfigure as flow velocity increases, where B is the slope of a double logarithmic plot of speed-specific drag (D/U^2, where D is drag and U is velocity) as a function of velocity; the greater the absolute value of the negative slope, the greater the relative drag reduction experienced
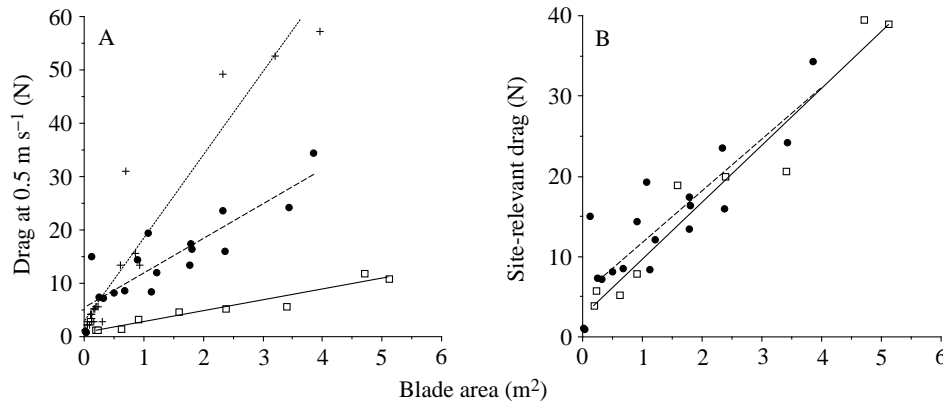
Fig. 6. (A) Drag (D, determined at $0.5\,\mathrm{m\,s^{-1}}$) as a function of blade area (A_B) for kelp from each site: protected (filled circles, dashed line, slope=7.0, P=0.0001, r^2=0.84), current-swept (open squares, solid line, slope=2.0, P=0.0001, r^2=0.94) and wavy (crosses, dotted line, slope=16, P=0.0001, r^2=0.92). ANCOVA revealed that slopes differ from each other (P<0.001); *a posteriori* pairwise comparisons using Tukey's Q revealed that all slopes differed significantly from each other (all P<0.05). (B) Site-relevant drag (D_s) as a function of blade area (A_B) for kelp from the protected site ($0.5\,\mathrm{m\,s^{-1}}$; filled circles, dashed line, slope=7.0, P=0.0001, r^2=0.84) and the current-swept site ($1.5\,\mathrm{m\,s^{-1}}$; open squares, solid line; slope=7.1, P=0.0001, r^2=0.94). ANCOVA revealed that neither slopes nor elevations differ significantly from each other (slopes, P>0.05; elevations, P>0.05). All slopes in this figure are uncorrected for error in measurement of blade area because the value obtained for κ was 0.999.

with an increase in velocity. We determined B for each individual kelp by calculating the slope of a linear regression of a plot of $\log(D/U^2)$ *versus* $\log U$. *N. luetkeana* from the protected site had significantly steeper values of B (mean B=−1.2, S.D.=0.28, N=16) than did those from the current-swept site (mean B=−0.85, S.D.=0.16, N=8) or the wavy site (mean B=−0.75, S.D.=0.25, N=19) (ANOVA and Fisher PLSD, P<0.05). These results are similar to those obtained by Armstrong (1989), who found for the kelp *Hedophyllum sessile* that ruffled individuals from a protected site had steeper values of B than did strap-like individuals from a more exposed site. In the case of *N. luetkeana*, the strap-like kelp from the current-swept site collapsed into streamlined bundles at lower velocities than did the ruffled kelp; therefore, the kelp with strap-like blades did not show as much drag reduction with further increases in velocity as did the ruffled kelp (which had much greater initial drag and which required higher water speeds to achieve passive streamlining). Our values for B are comparable with those reported for other macroalgae: *H. sessile* (−0.57 to −1.2; Armstrong, 1989), *Sargassum filipendula* (−1.06 to −1.47; Pentcheff, cited in Vogel, 1984); various species of small intertidal brown and red algae (−0.28 to −0.76; Carrington 1990); and freshwater red algae (−0.33 to −1.27; Sheath and Hambrook, 1988).

Kelp from all three sites showed a decrease in C_D as blade area increased (i.e. the bundles of blades on large kelp were more streamlined than those on small kelp) (Fig. 7). Since drag is proportional to the product of C_D and blade area, our data indicate that the
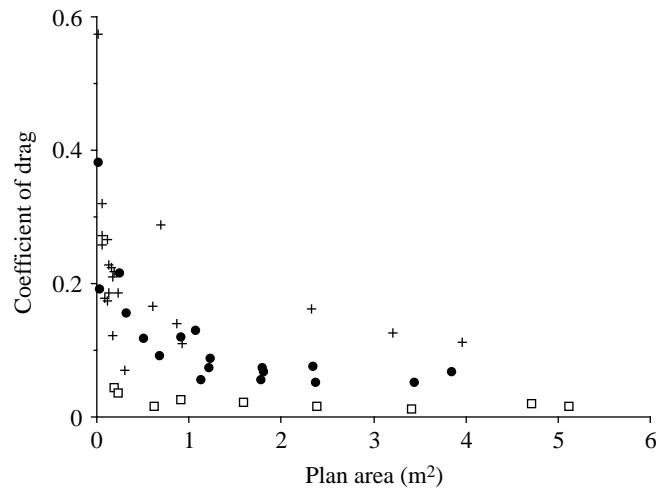
Fig. 7. Coefficient of drag (C_D) as a function of plan area (S) (see equation 1) for kelp from each site (linear regression statistics are for the lines determined from a double logarithmic regression of these data): protected (filled circles, slope=−0.33, $P<0.001$, $r^2=0.81$), current-swept (open squares, slope=−0.29, $p<0.003$, $r^2=0.74$) and wavy (crosses, slope=−0.21, $P<0.005$, $r^2=0.45$). ANCOVA revealed that while slopes are not significantly different from each other ($P>0.05$), elevations are significantly different ($P<0.001$); *a posteriori* pairwise comparisons using Tukey's Q revealed that all elevations differed significantly from each other (all $P<0.05$).

consequences for drag of growth in blade area are greater for small kelp than for large ones.

The total drag per kelp at a given velocity ($0.5 \, \mathrm{m \, s^{-1}}$) increased with blade area for kelp from all three sites, with the rate of increase being greatest for kelp from the wavy site and lowest for kelp from the current-swept site (Fig. 6A). Therefore, although blade area is a good predictor of the force that a *N. luetkeana* stipe must bear, the relationship of force to blade area also depends on the morphology of the blades, which is site-dependent.

Drag forces borne by stipes in different habitats

Not only do blade morphologies differ between sites, but ambient current velocities differ as well. In this study, we could only assess the forces on stipes of kelp from the sites subjected to unidirectional flow, since kelp from the wavy site can move *with* the flow and hence transmit little force to their stipes (see discussion of blade morphology above). When we considered drag at the relevant 'typical' peak velocity for each of the sites subjected to unidirectional currents ($0.5 \, \mathrm{m \, s^{-1}}$ at Shady Cove and $1.5 \, \mathrm{m \, s^{-1}}$ at Turn Rock; determination of typical peak velocities explained above in Materials and methods section on field sites), we found: (1) that the drag forces on kelp bearing similar blade areas were comparable at the two sites, and (2) that the rate of increase of drag with an increase in blade area did not differ between the sites (Fig. 6B). Therefore, the load that a *N. luetkeana* stipe must bear due to the drag on the blades is similar between different flow habitats because the kelp adjust their blade morphology.
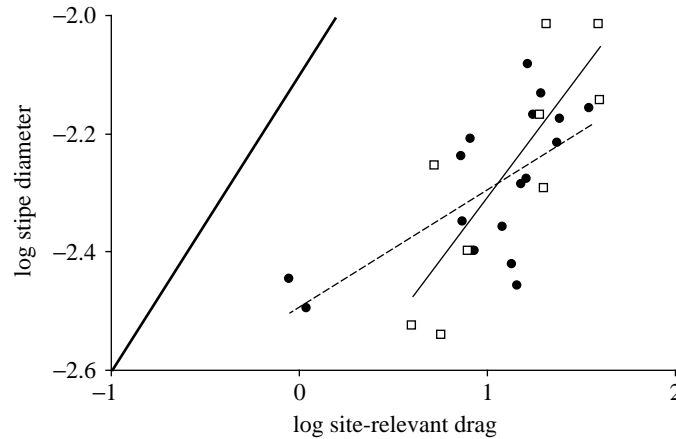
Fig. 8. Double logarithmic plot of stipe diameter (d) (in m) as a function of site-relevant drag (D_s) (in N) for kelp from the protected site ($0.5\,\text{m}\,\text{s}^{-1}$; filled circles, dashed line, slope=0.20, P=0.003, r^2=0.39) and the current-swept site ($1.5\,\text{m}\,\text{s}^{-1}$; open squares, thin solid line, slope=0.43, P=0.006, r^2=0.63). Whereas the slope for the best fitting line for the data from the current-swept site (thin solid line) does not significantly differ from 0.5 (the slope of the thick solid line) (P>0.05), the slope of the best fitting line for the data from the protected site (dashed line) is significantly less than 0.5 (P<0.05).

The relationship of stipe diameter (d) to site-relevant drag (drag at the water velocity relevant to that site, D_s) is plotted in Fig. 8 for kelp from the sites exposed to unidirectional flow. For elastic similarity and for stress similarity, we would expect $d \propto D_s^{0.5}$ if material properties were constant (Peterson *et al.* 1982). Indeed, for kelp from the current-swept site, the relationship of d to D_s is not significantly different from $d \propto D_s^{0.5}$ (statistics reported in Fig. 8). However, for kelp from the protected site, $d \propto D_s^{0.2}$, which is significantly different from the expectation for elastic or stress similarity *if* we assume that stipe material properties are constant. In the next section, we shall examine this assumption.

Material properties

A typical stress/extension ratio curve (σ/λ curve) for *N. luetkeana* stipe tissue is given in Fig. 2, and the material properties for stipe tissues from the three sites are summarized in Table 2. Our measurements of stipe material properties are consistent with those reported by Koehl and Wainwright (1977) for *N. luetkeana*. This kelp's stipe tissue is stiffer at low extension ratios (λ) than at high values of λ, with the transition in modulus (from E_1 to E_2) beginning at λ values in the range 1.1–1.2. The stipe tissues of another kelp, *Postelsia palmaeformis*, also have σ/λ curves of this shape (Holbrook *et al.* 1991).

When *N. luetkeana* stipe tissue was pulled to λ values within the E_1 range, it was very resilient ($W_{\text{recoil}}/W_{\text{pull}}$=0.93, s.d.=0.06, N=6) and maintained stress until it was returned to its resting length (Fig. 3A). The high resilience of *N. luetkeana* stipes at λ values in the E_1 region permits them to snap back to resting length between bursts of high force (see discussion below of *N. luetkeana* as shock absorbers).

In contrast, stipe tissue pulled to λ values in the E_2 range was significantly less resilient (W_{recoil}/W_{pull}=0.52, s.d.=0.05, N=19; t-test, P=0.0001), and stress in the tissue dropped to zero before the specimens were fully returned to resting length (Fig. 3B). Vincent and Gravell (1986) also found hysteresis when they pulled *Laminaria* blade tissues to high extensions. Although highly resilient materials (such as *N. luetkeana* tissue in the E_1 region of its σ/λ curve) are brittle because they store strain energy that can be readily transferred to an advancing crack (see Biedka *et al.* 1987; Denny *et al.* 1989; Vincent, 1990; Holbrook *et al.* 1991), the reduced resilience of *N. luetkeana* stipe in the E_2 range of its σ/λ curve may lessen such susceptibility to brittle failure. Furthermore, the plastic deformation and great extensibility of *N. luetkeana* stipe tissue in the E_2 region of its σ/λ curve may help to blunt the tips of cracks, which should reduce local stresses at the crack tips (Gordon, 1968). Indeed, crack-tip blunting has been shown to reduce susceptibility to brittle failure in the blades of the red macroalga *Iridaea flaccida* (Denny *et al.* 1989).

The low elastic moduli (E values) and breaking stresses (σ_{brk} values) we measured for *N. luetkeana* stipes (Table 2) are comparable with those of stipe and blade tissues of other brown and red macroalgae (Delf, 1932; Charters *et al.* 1969; Koehl, 1982, 1986; Vincent and Gravell, 1986; Armstrong, 1987; Denny *et al.* 1989; Carrington, 1990; Holbrook *et al.* 1991; Lowell *et al.* 1991; Dudgeon and Johnson, 1992). Although the breaking extensions (λ_{brk} values) of *N. leutkeana* stipes are at the high end of the range reported for other species of macroalgae (Koehl, 1986; Armstrong, 1987; Sheath and Hambrook, 1988; Denny *et al.* 1989; Holbrook *et al.* 1991), the work per volume (W/V) required to break *N. luetkeana* stipes is slightly lower than that measured for other kelp (Holbrook *et al.* 1991; Lowell *et al.* 1991). When compared with other biomaterials, the stipe tissues of *N. luetkeana* and other species of macroalgae are neither stiff nor strong (i.e. they have low E values and σ_{brk} values; Wainwright *et al.* 1976; Koehl, 1986; Denny *et al.* 1989), nor are algal tissues tough (i.e. they have low tearing energy; Vincent, 1990; Denny *et al.* 1989). However, the high extensibility (i.e. high λ_{brk}) of algal stipes renders these structures able to absorb a lot of strain energy before failing (i.e. they have relatively high values of W/V when compared with other biomaterials; Wainwright *et al.* 1976; Koehl, 1986).

Comparisons of Nereocystis luetkeana *from different sites*

The results of an ANOVA comparing material properties of stipes from *N. luetkeana* from the different sites are summarized in Table 2. Stipe tissues of kelp collected during the summer from the protected site were significantly stronger (σ_{brk}) than were those from the current-swept and wavy sites. Although there was no significant difference in breaking extension ratio (λ_{brk}) between sites, the work per volume required to break a stipe was higher for the protected kelp than for those from the other two sites. Stipes from the protected habitat were stiffer at low extensions (E_1) than were those from the other sites, whereas at higher extensions (E_2), stipes from both the protected and current-swept habitats were stiffer than stipes from the wavy habitat. Because our results indicate that the material properties of *N. luetkeana* can differ between sites, we cannot assume a single value for such variables as modulus or strength when conducting allometric analyses for kelp from different habitats.

Table 3. *Kendall's τ (rank correlation coefficient) was used to determine association between blade area and mechanical variables of* Nereocystis luetkeana

Variable	Symbol	Site		
		Protected	Wavy	Current-swept
Breaking stress (MN m^{-2})	σ_{brk}	None (7) None (11)	None (17)	None (9)
Breaking extension ratio	λ_{brk}	None (7) None (11)	Positive (17)	None (9)
Stiffness 1 (MN m^{-2})	E_1	None (7) None (11)	None (22)	None (9)
Stiffness 2 (MN m^{-2})	E_2	None (7) None (11)	None (18)	None (9)
Work to break per volume (MJ m^{-3})	W/V	None (7) None (11)	None (16)	None (9)
Total work to break kelp (kJ)	W	None (7) None (11)	*	Positive (9)

Positive means that there was a significantly positive association ($P<0.05$) and None means that there was no association ($P>0.05$) between blade area and the mechanical variable.

For the protected site, separate results for the months of August (listed first) and September (listed second) are given.

*W could not be calculated for kelp from the wavy site because data on the volume of the stipe tissue were not available (see Table 1).

Values in parentheses are number of kelp.

Other species of kelp also show differences in material properties in different water-flow habitats (Charters *et al.* 1969; Armstrong 1987; McEacheron and Thomas, 1987). Furthermore, several studies have shown that such changes in kelp material properties can be environmentally induced (Kraemer and Chapman, 1991; Lowell *et al.* 1991).

Relationship of material properties to thallus size

There was no correlation between the various material properties of stipe tissues we measured and the blade areas (a mechanically relevant measure of thallus size) of the *N. luetkeana* kelp from which they were taken (Table 3). The only exception to this was the positive association between breaking extension ratio and blade area for the kelp from the wavy site. However, this result could have been due to chance, since the $P<0.05$ criterion for significance implies that one out of twenty comparisons may yield a correlation simply due to chance alone (we ran twenty statistical tests and found only one significant association). Therefore, the assumption that *N. luetkeana* stipe tissue properties remain constant as the kelp grow appears to be valid (although as kelp age and become damaged in autumn their material properties deteriorate, as described above).

Scaling of Nereocystis leutkeana *in different water-flow habitats*

Since stipe material properties, blade morphology and ambient flow conditions differ between habitats for *N. luetkeana*, we must consider the stresses and extensions experienced by stipes *in nature* to evaluate the mechanical consequences of size. At site-
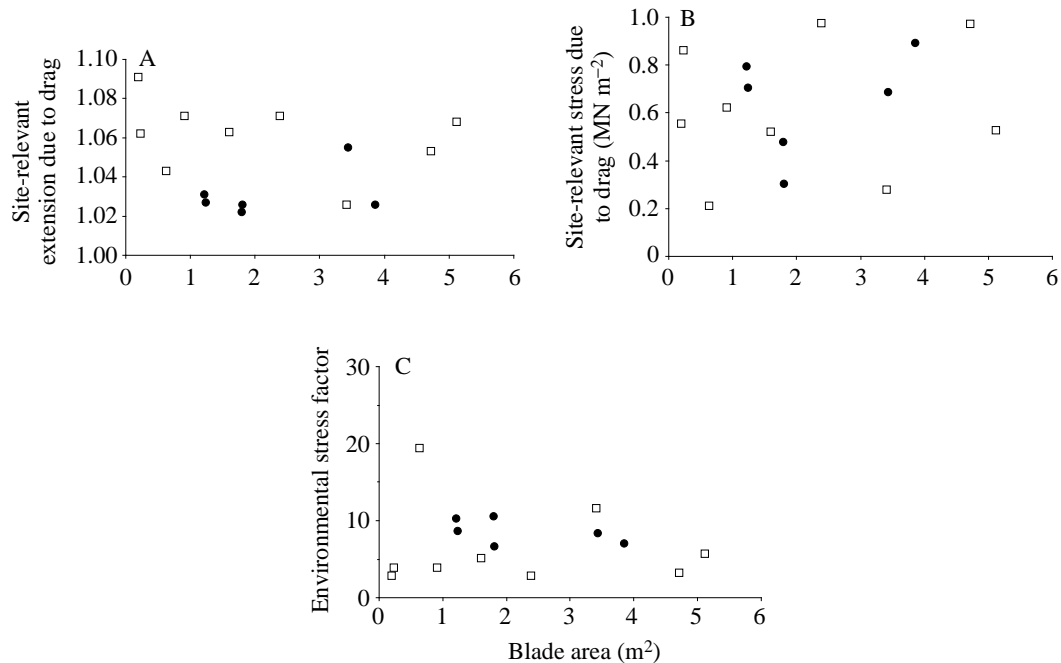
Fig. 9. (A) Extension due to drag (λ_{drag}), (B) stress due to drag (σ_{drag}) and (C) environmental stress factor ($\sigma_{brk}/\sigma_{drag}$) determined for individual kelp at site-relevant velocities (protected summer at $0.5\,\mathrm{m\,s^{-1}}$, filled circles; current-swept at $1.5\,\mathrm{m\,s^{-1}}$, open squares) and plotted as a function of blade area. Kendall's τ (rank correlation coefficient) revealed that, in all cases, these site-relevant characters were independent of blade area (all $P>0.19$). The smallest kelp (blade area=$0.032\,\mathrm{m^2}$) was omitted from these analyses because of the anomalous morphology of such juvenile kelp. The environmental stress factor of this juvenile kelp was more than 30 % higher than that measured for any other kelp in this study.

relevant peak velocities, σ_{drag} and λ_{drag} did not change with size (Fig. 9A,B). However, although stress due to site-relevant drag (σ_{drag}) did not differ between sites, extension ratio due to site-relevant drag (λ_{drag}) was greater at the current-swept site than at the protected site (Table 2).

Peak stresses in the stipes of *N. luetkeana* are maintained, not by allometric scaling of stipe dimensions, but rather by adjustments in blade morphology in different flow habitats. Therefore, we see within this species of kelp a phenomenon analogous to the 'dynamic strain similarity' (*sensu* Rubin and Lanyon, 1984) between species of vertebrate animals: peak stresses in the bones of vertebrates representing a range of body sizes are maintained, not entirely by allometric scaling of bone dimensions, but rather by the use of more gentle gaits by large animals. Vertebrates (for which the loads on limb bones are mainly due to locomotion) can adjust their behavior, whereas kelp (for which the loads on stipes are mainly due to environmental hydrodynamic forces) can adjust their morphology. Similarly, sessile animals subjected to hydrodynamic forces can alter the magnitude of those forces by shape changes due to growth (e.g. Hunter, 1988) or behavior (Koehl, 1977). Spiders provide another example of how an organism's behavior can

compensate for an insufficiently robust support structure: although the drag line is not strong enough to bear the force of a falling spider, the ability of the animal to draw drag-line silk from its spinnerets during a fall absorbs enough energy to prevent breakage of the drag line (Brandwood, 1985). All these examples of dynamic strain similarity illustrate the importance of determining the mechanical loads on structures *as they are used by organisms in nature*.

Nereocystis luetkeana *kelp as shock absorbers*

N. luetkeana can be subjected to short (<1 s) pulses of rapid water flow in the turbulent currents they encounter in both protected and exposed habitats (Koehl and Wainwright, 1977; Koehl and Alberte, 1988). The low modulus of the stipes of these kelp permits them to 'give' when subjected to a burst of high drag (Koehl and Wainwright, 1977; Koehl, 1984, 1986). We found that *N. luetkeana* stipes in the field operate in the E_1 range of their stress/extension ratio curves (all 37 tests for nine kelp from the current-swept site and all 72 tests for eight summer kelp from the protected site), where the tissues have very high resilience (Fig. 3A). This high resilience permits them to snap back to resting length before the next pulse of high force. In contrast, some deteriorating autumn kelp operated in the E_2 region of their stress/extension ratio curves (four out of 11 kelp tested, eight out 37 mechanical tests), where their resilience is lower (Fig. 3B).

The ability of a *N. luetkeana* to withstand transient high forces without breaking depends on the mechanical work required to break the stipe. There are two mechanisms by which the performance of a stipe as a 'shock-absorber' can be improved: the tissues can require a high work per volume (W/V) for breakage or the stipe can be long (i.e. the total volume of tissue absorbing the strain energy is large). There was no significant difference in the length (which depends on water depth; Duncan, 1973) or total tissue volume of the stipes from the protected and the current-swept sites (Table 1) but, because the protected stipes had a higher W/V, the total work required to break healthy summer kelp was higher at this site than at the current-swept site (Table 2). Although *N. luetkeana* from the shallow wavy site had the same W/V as the current-swept kelp (Table 2), we would expect these shorter kelp from shallow water to be less effective shock-absorbers than the longer *N. luetkeana* from the other two deeper sites. It is interesting to note that at the current-swept site there was a positive association between the total work required to break the stipes (W) and the blade area (A_B) that the stipes supported (Table 3).

Environmental stress factors

The environmental stress factor of a component of an individual organism at a particular stage in its life is the ratio of the breaking stress of that component to the peak stress that it experiences at that stage in its habitat. In the case of *N. luetkeana,* we used stipe breaking stress (σ_{brk}) and the stress due to drag (σ_{drag}) at the peak site-relevant velocity (defined above) to calculate environmental stress factor for each kelp from the current-swept and the protected sites (the sites exposed to unidirectional currents). Environmental stress factor was independent of site (Table 2) and of blade area (Fig. 9C), suggesting that the blade morphology, stipe diameter and tissue properties of

N. luetkeana were scaled in such a way that environmental stress factor was maintained between habitats and as the kelp grew.

Although a biological structure with a high environmental stress factor has a reduced probability (P) of breaking, there is often some cost (C_s) associated with producing and using that less-breakable structure. Alexander (1981, 1988) considered this issue for safety factor and proposed that the optimal safety factor for a biological structure is one that minimizes the function Φ, where:

$$\Phi = PC_f + C_s,\qquad(8)$$

where C_f is the cost of failure. In a similar way, we can consider the environmental stress factor for *N. luetkeana*, using reproductive output (spore production) as a measure of cost that relates more directly to fitness than does energy. Although spore production rates have not been quantified for *N. luetkeana,* we can consider C_f and C_s in qualitative terms.

Cost of failure (C_f). We might imagine the cost of stipe failure to be high for *N. luetkeana* because they do not regrow from the remaining stumps. However, since the bulk of *N. luetkeana* spore production occurs during the late summer (Rigg, 1917), C_f should decline during the autumn and winter. Indeed, we found that although *N. luetkeana* were scaled such that their environmental stress factors (and hence, P) were maintained during the summer, their environmental stress factors became significantly lower in the autumn (Table 2). Although this is consistent with the predictions of Alexander's theory, this decrease in strength may simply reflect the accumulation of flaws in the stipes over time rather than an optimization of the environmental stress factor. The possible benefits of breakage should also be considered: broken *N. luetkeana* can continue to photosynthesize (Koehl and Alberte, 1988), grow and release sori (M. A. R. Koehl, unpublished data). As long as their pneumatocysts (Fig. 1A) are not damaged, broken *N. luetkeana* can remain afloat for days and are commonly seen drifting in currents in the field. Such breakage and drifting may be an important mechanism of dispersal for these kelp.

Cost of maintaining the environmental stress factor (C_s). *N. luetkeana* maintain the environmental stress factor, in part, by the streamlining of blades. Such streamlining reduces photosynthetic rate due to self-shading as moving water pushes the strap-like blades on top of each other into a bundle (Koehl and Alberte, 1988). Reduced photosynthesis should translate into reduced blade growth rate and, hence, into a lowering of spore production rate. Furthermore, trade-offs between tissue strength and photosynthesis have been noted for other species of macroalgae (reviewed by Koehl, 1986); however, such costs have not been assessed yet for *N. luetkeana.*

In contrast to *N. leutkeana*, which maintain their environmental stress factor as they increase in size during the summer, several species of intertidal red algae show a decrease in this factor with increasing size (Carrington, 1990; Dudgeon and Johnson, 1992). Unlike *N. luetkeana*, these red algae can regenerate from their holdfasts after breakage; hence, their cost of failure (C_f) might be expected to be lower. Moreover, among these red algae, a species that regenerates slowly, *Mastocarpus stellatus,* has a higher environmental stress factor than does a co-occurring species, *Chondrus crispus,* that

regenerates more quickly (i.e. that may have a lower C_f) but that is broken more frequently (and therefore has a higher P) in winter storms (Dudgeon and Johnson, 1992). Koehl (1984, 1986) has noted a similar pattern among kelp species, where those with weak tissues tend to have life histories characterized by rapid growth, early reproduction and susceptibility to seasonal dislodgment. Although these observations are consistent with the predictions of Alexander's (1981, 1988) theory, we cannot evaluate whether they represent optimization of the environmental stress factor until the reproductive output or success of these macrophytes has been quantified.

Conclusions

We have investigated the mechanical scaling of *Nereocystis luetkeana,* a giant kelp whose stipes are loaded in tension due to hydrodynamic forces on the blades of the kelp. If we simply consider the allometry of the morphological characters of these kelp, we conclude that the stipes are underscaled relative to the blade area they support (i.e. that the kelp do not maintain stress or elastic similarity as they grow). However, we must examine the assumptions underlying such an allometric analysis: (1) that load on a support structure (the stipe) is simply proportional to a morphological feature (blade area), and (2) that material properties of the stipe are constant. We found that kelp alter their blade morphologies (hence their drag coefficients) and their stipe material properties in different hydrodynamic environments such that they maintain elastic similarity and environmental stress factor as they grow. Thus, sessile organisms such as these kelp can, *via* their growth responses to environmental stresses, show dynamic strain similarity. Our study illustrates the importance of moving beyond simple allometric analyses of the mechanical support structures of organisms: if we are to understand the functional consequences of changes in organism size, we must also measure how organisms actually perform *in the field* in different habitats.

References

ABBOTT, I. A. AND HOLLENBERG, G. J. (1976). *Marine Algae of California.* Stanford, CA: Stanford University Press.

ALEXANDER, R. McN. (1971). *Size and Shape.* London, England: Edward Arnold.

ALEXANDER, R. McN. (1981). Factors of safety in the structure of animals. *Sci. Prog.* **67**, 109–130.

ALEXANDER, R. McN. (1988). The scope and aims of functional and ecological morphology. *Neth. J. Zool.* **38**, 3–22.

AMSLER, C. D. AND NEUSHUL, M. (1991). Photosynthetic physiology and chemical composition of spores of the kelps *Macrocystis pyrifera, Nereocystis luetkeana, Laminaria farlowii* and *Pterygophora californica* (Phaeophyceae). *J. Phycol.* **27**, 26–34.

ARMSTRONG, S. L. (1987). Mechanical properties of the tissues of the brown alga *Hedophyllum sessile* (C. Ag.) Setchell: variability with habitat. *J. exp. mar. Biol. Ecol.* **114**, 143–151.

ARMSTRONG, S. L. (1989). The behavior in flow of the morphologically variable seaweed *Hedophyllum sessile* (CAG) Setchell. *Hydrobiol.* **183**, 115–122.

BANSE, K. AND MOSHER, S. (1980). Adult body mass and annual production/biomass relationships for field populations. *Ecol. Monogr.* **50**, 355–379.

BIEDKA, R. F., GOSLINE, J. M. AND WREEDE, R. E. D. (1987). Biomechanical analysis of wave-induced mortality in the marine alga *Pterygophora californica. Mar. Ecol. Prog. Ser.* **36**, 163–170.

BONNER, J. T. (1968). Size change in development and evolution. In *Paleobiological Aspects of Growth and Development. Paleontological Society Memoir* **2** (ed. D. B. Macurda), pp. 1–15. Tulsa: Economic Palaeontologists and Mineralogists.

BRANDWOOD, A. (1985). Mechanical properties and factors of safety of spider drag-lines. *J. exp. Biol.* **116**, 141–151.

CALDER, W. A. (1984). *Size, Function and Life History.* Cambridge, MA: Harvard University Press.

CARRINGTON, E. (1990). Drag and dislodgment of an intertidal macroalga: consequences of morphological variation in *Mastocarpus papillatus* Kützing. *J. exp. mar. Biol. Ecol.* **139**, 185–200.

CHARTERS, A. C., NEUSHUL, M. AND BARILOTTI, C. (1969). The functional morphology of *Eisenia arborea. Proc. int. Seaweed Symp.* **6**, 89–105.

CHATFIELD, C. AND COLLINS, A. J. (1980). *Introduction to Multivariate Analysis.* London: Chapman and Hall.

CURREY, J. (1984). *The Mechanical Adaptations of Bones.* Princeton: Princeton University Press.

DELF, E. M. (1932). Experiments with the stipes of *Fucus* and *Laminaria. J. exp. Biol.* **9**, 300–313.

DENNY, M. W. (1988). *Biology and the Mechanics of the Wave-Swept Environment.* Princeton, NJ: Princeton University Press.

DENNY, M. W. (1991). Biology, natural selection and the prediction of maximal wave-induced forces. *S. Afr. J. mar. Sci.* **10**, 353–363.

DENNY, M. W., BROWN, V., CARRINGTON, E., KRAEMER, G. AND MILLER, A. (1989). Fracture mechanics and the survival of wave-swept macroalgae. *J. exp. mar. Biol. Ecol.* **127**, 211–228.

DENNY, M. W., DANIEL, T. L. AND KOEHL, M. A. R. (1985). Mechanical limits to size in wave-swept organisms. *Ecol. Monogr.* **55**, 69–102.

DENNY, M. W. AND GAINES, S. (1990). On the prediction of maximal intertidal wave forces. *Limnol. Oceanogr.* **35**, 1–15.

DUDGEON, S. R. AND JOHNSON, A. S. (1992). Thick *versus* thin: Thallus morphology and tissue mechanics influence differential drag and dislodgement of two co-dominant seaweeds. *J. exp. mar. Biol. Ecol.* **165**, 23–43.

DUNCAN, M. J. (1973). *In situ* studies of growth and pigmentation of the phaeophycean *Nereocystis luetkeana. Helgolander wiss. Meeresunter.* **24**, 510–525.

DUNCAN, M. J. AND FOREMAN, R. E. (1980). Phytochrome-mediated stipe elongation in the kelp *Nereocystis* (Phaeophyceae). *J. Phycol.* **16**, 138–142.

ETTER, R. J. (1988). Asymmetrical developmental plasticity in an intertidal snail. *Evolution* **42**, 322–334.

FOREMAN, R. E. (1970). Physiology, ecology and development of the brown alga *Nereocystis luetkeana* (Mertens) P&R. PhD thesis, University of California, Berkeley.

FULLER, W. A. (1987). *Measurement Error Models.* New York: John Wiley and Sons.

GERARD, V. A. (1987). Hydrodynamic streamlining of *Laminaria saccharina* Lamour in response to mechanical stress. *J. exp. mar. Biol. Ecol.* **107**, 237–244.

GORDON, J. E. (1968). *The New Science of Strong Materials.* Baltimore: Penguin Books Inc.

GOULD, S. J. (1966). Allometry in Pleistocene land snails from Bermuda: the influence of size upon shape. *J. Paleont.* **40**, 1131–1141.

GUTIERREZ, L. M. AND FERNANDEZ, C. (1992). Water motion and morphology in *Chondrus crispus* (Rhodophyta). *J. Phycol.* **28**, 156–162.

HARVEY, P. H. AND PAGEL, M. D. (1991). *The Comparative Method in Evolutionary Biology.* Oxford: Oxford University Press.

HAWKES, M. W. (1981). *Porphyra nereocystis* and *P. thuretti* (Rhodophyta): Gametophyte morphology, distribution and occurrence. *Syeis* **14**, 97–108.

HOLBROOK, N. M., DENNY, M. W. AND KOEHL, M. A. R. (1991). Intertidal 'trees': consequences of aggregation on the mechanical and photosynthetic properties of sea palms *Postelsia palmaeformis* Ruprecht. *J. exp. mar. Biol. Ecol.* **146**, 39–67.

HUNTER, T. (1988). Mechanical design of hydroids: flexibility, flow forces, and feeding in *Obelia longissima.* PhD thesis, University of California, Berkeley.

HURD, A. M. (1916). Factors influencing the growth and distribution of *Nereocystis luetkeana. Puget Sound mar. Sta. Pub.* **1**, 185–197.

JACKELMAN, J. J. AND BOLTON, J. J. (1990). Form variation and productivity of an intertidal foliose *Gigartina* species (Rhodophyta) in relation to wave exposure. *Hydrobiologia* **204/205**, 57–64.

KOEHL, M. A. R. (1977). Effects of sea anemones on the flow forces they encounter. *J. exp. Biol.* **69**, 87–105.

KOEHL, M. A. R. (1982). The interaction of moving water and sessile organisms. *Scient. Am.* **247**, 124–134.

KOEHL, M. A. R. (1984). How do benthic organisms withstand moving water? *Am. Zool.* **24**, 57–70.

KOEHL, M. A. R. (1986). Seaweeds in moving water: Form and mechanical function. In *On the Economy of Plant Form and Function* (ed. T. J. Givnish), pp. 603–734. Cambridge, England: Cambridge University Press.

KOEHL, M. A. R. AND ALBERTE, R. S. (1988). Flow, flapping and photosynthesis of *Nereocystis luetkeana:* A functional comparison of undulate and flat blade morphologies. *Mar. Biol.* **99**, 435–444.

KOEHL, M. A. R., HUNTER, T. AND JED, J. (1991). How do flexibility and length affect hydrodynamic forces on sessile organisms in waves *versus* in currents? *Am. Zool.* **31**, 60A.

KOEHL, M. A. R. AND WAINWRIGHT, S. A. (1977). Mechanical adaptations of a giant kelp. *Limnol. Oceanogr.* **22**, 1067–1071.

KOEHL, M. A. R. AND WAINWRIGHT, S. (1985). Biomechanics. In *Handbook of Phycological Methods* (ed. M. M. Littler and D. S. Littler), pp. 291–313. Cambridge, England: Cambridge University Press.

KRAEMER, G. P. AND CHAPMAN, D. J. (1991). Biomechanics and alginic acid composition during hydrodynamic adaptation by *Egregia menziesii* (Phaeophyta) juveniles. *J. Phycol.* **27**, 47–53.

LABARBERA, M. (1985). Mechanical properties of a North American aboriginal fishing line: The technology of a natural product. *Am. Anthropol.* **87**, 625–636.

LABARBERA, M. (1989). Analyzing body size as a factor in ecology and evolution. *A. Rev. ecol. Syst.* **20**, 97–117.

LOWELL, R. B., MARKHAM, J. H. AND MANN, K. H. (1991). Herbivore-like damage induces increased strength and toughness in a seaweed. *Proc. R. Soc. Lond.* **243**, 31–38.

MARKHAM, J. W. (1969). Vertical distribution of epiphytes on the stipe of *Nereocystis luetkeana* (Mertens) Postels and Ruprecht. *Syesis* **2**, 227–240.

MCEACHREON, J. C. T. AND THOMAS, M. L. H. (1987). Attachment strength of *Ascophyllum nodosum* (L.) LeJolis and exposure to wave action. *Bot. mar.* **30**, 217–222.

MCMAHON, T. (1973). Size and shape in biology. *Science* **179**, 1201–1204.

MCMAHON, T. (1975). Using body size to understand the structural design of animals: quadrupedal locomotion. *J. appl. Physiol.* **39**, 619–627.

MCMAHON, T. A. AND BONNER, J. T. (1983). *On Size and Life*. New York, NY: W. H. Freeman and Company.

MILLER, K. A. AND ESTES, J. A. (1989). Western range extension for *Nereocystis luetkeana* in the North Pacific Ocean. *Bot. mar.* **32**, 535–538.

NATIONAL OCEANIC AND ATMOSPHERIC ADMINISTRATION (1981). *Tidal Current Tables, Pacific Coast of North America and Asia.* Rockville, MD: US Department of Commerce, National Oceanic and Atmospheric Administration, National Ocean Survey.

NICHOLSON, N. L. (1970). Field studies on the giant kelp *Nereocystis*. *J. Phycol.* **6**, 177–182.

NIKLAS, K. J. (1992). *Plant Biomechanics: An Engineering Approach to Plant Form and Function.* Chicago: The University of Chicago Press.

NORTON, T. A. (1986). The ecology of macroalgae in the Firth of Clyde. *Proc. R. Soc. Edin.* **90**B, 255–269.

PALUMBI, S. R. (1984). Tactics of acclimation: morphological changes of sponges in an unpredictable environment. *Science* **225**, 1478–1480.

Patterson, M. R. (1992). A mass transfer explanation of metabolic scaling relations in some aquatic invertebrates and algae. *Science* **255**, 1421–1423.

Pedley, T. J. (1977). *Scale Effects in Animal Locomotion*. New York, NY: Academic Press.

Peters, R. (1913). A preliminary study of the causes that produce 'bald-headed' kelp. *Kansas Univ. Sci. Bull.* **9**, 3–10.

Peters, R. H. (1983). *The Ecological Implications of Body Size*. Cambridge, England: Cambridge University Press.

Peterson, J. A., Benson, J. A., Ngai, M., Morin, J. and Ow, C. (1982). Scaling in tensile 'skeletons': structures with scale-independent length dimensions. *Science* **217**, 1267–1270.

Reiss, M. J. (1989). *The Allometry of Growth and Reproduction*. Cambridge, England: Cambridge University Press.

Rice, E. L., Kenchington, T. J. and Chapman, A. R. O. (1985). Intraspecific geographic–morphological variation patterns in *Fucus distichus* and *F. evanescens*. *Mar. Biol.* **88**, 207–215.

Rigg, G. B. (1917). Seasonal development of bladder kelp. *Puget Sound mar. Sta. Pub.* **1**, 309–318.

Rosell, K.-G. and Srivastava, L. M. (1984). Seasonal variation in the chemical constituents of the brown algae *Macrocystis integrifolia* and *Nereocystis luetkeana*. *Can. J. Bot.* **62**, 2229–2236.

Rubin, C. T. and Lanyon, L. E. (1984). Dynamic strain similarity in vertebrates: an alternative to allometric limb bone scaling. *J. theor. Biol.* **107**, 321–327.

Schmidt-Nielsen, K. (1974). Scaling in biology: The consequences of size. *Exp. Zool.* **194**, 287–308.

Schmidt-Nielsen, K. (1984). *Scaling: Why is Animal Size so Important?* Cambridge, England: Cambridge University Press.

Sheath, R. G. and Hambrook, J. A. (1988). Mechanical adaptations to flow in freshwater red algae. *J. Phycol.* **24**, 107–111.

Stanley, S. M. (1973). An explanation for Cope's rule. *Evolution* **27**, 1–26.

Tateno, M. and Bae, K. (1990). Comparison of lodging safety factor of untreated and succinic acid 2,2-dimethylhydrazide-treated shoots of mulberry tree. *Plant Physiol.* **92**, 12–16.

Vadas, R. L. (1972). Ecological implications of culture studies on *Nereocystis luetkeana*. *J. Phycol.* **8**, 196–203.

Vincent, J. (1990). *Structural Biomaterials*. Princeton, NJ: Princeton University Press.

Vincent, J. F. V. and Gravell, K. (1986). The mechanical design of kelp, *Laminaria digitata*. *J. Materials Sci. Lett.* **5**, 353–354.

Vogel, S. (1984). Drag and flexibility in sessile organisms. *Am. Zool.* **24**, 37–44.

Wainwright, S. A. (1970). Design in hydraulic organisms. *Naturwissenschaften* **57**, 321–326.

Wainwright, S. A., Biggs, W. D., Currey, J. D. and Gosline, J. M. (1976). *Mechanical Design in Organisms*. London: Edward Arnold

Wheeler, W. N., Smith, R. G. and Srivastava, L. M. (1984). Seasonal photosynthetic performance of *Nereocystis luetkeana*. *Can. J. Bot.* **62**, 664–670.